1-7-2015

Attentional filtering of visual information by neuronal ensembles in the primate lateral prefrontal cortex.

Sébastien Tremblay
Cognitive Neurophysiology Laboratory, Department of Physiology, McGill University, Montreal, QC H3G 1Y6, Canada & Integrated Program in Neuroscience, Montreal Neurological Institute, McGill University, Montreal, QC H3A 2B4, Canada

Florian Pieper
Institute for Neuro- & Pathophysiology, University Medical Center Hamburg-Eppendorf, 20246 Hamburg, Germany

Adam Sachs
Division of Neurosurgery, Department of Surgery, The Ottawa Hospital Research Institute, University of Ottawa, Ottawa, ON K1Y 4E9, Canada

Julio Martinez-Trujillo
Cognitive Neurophysiology Laboratory, Department of Physiology, McGill University, Montreal, QC H3G 1Y6, Canada & Robarts Research Institute, Departments of Psychiatry, Physiology and Pharmacology, Western University, London, ON N6A 5C1, Canada, julio.martinez@robarts.ca

Article

Neuron

Attentional Filtering of Visual Information by Neuronal Ensembles in the Primate Lateral Prefrontal Cortex

Highlights

- Neuronal ensembles in LPFC promptly filter visual information
- Noise correlations hinder attentional filtering by LPFC ensembles
- Neuronal ensembles' activity is resilient to distractor interference
- Ensemble coding is stable over the course of multiple weeks

Authors

Sébastien Tremblay, Florian Pieper, Adam Sachs, Julio Martinez-Trujillo

Correspondence

julio.martinez@robarts.ca

In Brief

In complex environments, the brain must focus attention on behaviorally relevant objects on a moment-by-moment basis. In this study, Tremblay et al. show that ensembles of neurons in the primate prefrontal cortex efficiently support this important function.

Tremblay et al., 2015, Neuron *85*, 202–215
January 7, 2015
http://dx.doi.org/10.1016/j.neuron.2014.11.021

CellPress

CellPress

Neuron
Article

Attentional Filtering of Visual Information by Neuronal Ensembles in the Primate Lateral Prefrontal Cortex

Sébastien Tremblay,[1,2] Florian Pieper,[3] Adam Sachs,[4] and Julio Martinez-Trujillo[1,5,*]
[1]Cognitive Neurophysiology Laboratory, Department of Physiology, McGill University, Montreal, QC H3G 1Y6, Canada
[2]Integrated Program in Neuroscience, Montreal Neurological Institute, McGill University, Montreal, QC H3A 2B4, Canada
[3]Institute for Neuro- & Pathophysiology, University Medical Center Hamburg-Eppendorf, 20246 Hamburg, Germany
[4]Division of Neurosurgery, Department of Surgery, The Ottawa Hospital Research Institute, University of Ottawa, Ottawa, ON K1Y 4E9, Canada
[5]Robarts Research Institute, Departments of Psychiatry, Physiology and Pharmacology, Western University, London, ON N6A 5C1, Canada
*Correspondence: julio.martinez@robarts.ca
http://dx.doi.org/10.1016/j.neuron.2014.11.021

SUMMARY

The activity of neurons in the primate lateral prefrontal cortex (LPFC) is strongly modulated by visual attention. Such a modulation has mostly been documented by averaging the activity of independently recorded neurons over repeated experimental trials. However, in realistic settings, ensembles of simultaneously active LPFC neurons must generate attentional signals on a single-trial basis, despite the individual and correlated variability of neuronal responses. Whether, under these circumstances, the LPFC can reliably generate attentional signals is unclear. Here, we show that the simultaneous activity of neuronal ensembles in the primate LPFC can be reliably decoded to predict the allocation of attention on a single-trial basis. Decoding was sensitive to the noise correlation structure of the ensembles. Additionally, it was resilient to distractors, predictive of behavior, and stable over weeks. Thus, LPFC neuronal ensemble activity can reliably encode attention within behavioral timeframes, despite the noisy and correlated nature of neuronal activity.

INTRODUCTION

The primate brain has a limited capacity to process the immense amount of visual information entering the visual system at any given moment (Marois and Ivanoff, 2005). Visual attention provides a solution to this problem by selecting behaviorally relevant information for detailed processing while filtering out distracting information (Petersen and Posner, 2012; Posner, 1980). In macaque monkeys, attention enhances the responses of visual neurons representing the sensory attributes of behaviorally relevant stimuli while suppressing the responses of neurons representing the attributes of irrelevant distractors (Desimone and Duncan, 1995; Moran and Desimone, 1985; Noudoost et al., 2010). During the voluntary allocation of attention, this response modulation is stronger and occurs earlier in the lateral prefrontal cortex relative to upstream striate and extrastriate visual areas (Buschman and Miller, 2007; Suzuki and Gottlieb, 2013; but see Katsuki and Constantinidis, 2012). Furthermore, activation (Moore and Fallah, 2004; Schafer and Moore, 2011) or inactivation (Monosov and Thompson, 2009; Noudoost and Moore, 2011) of prefrontal neurons increases or decreases, respectively, the modulation of single-neuron activity in visual cortices. This suggests that the primate LPFC contains a saliency map influencing neuronal activity in visual cortical areas, thus playing an instrumental role in visual selective attention (Miller and Cohen, 2001; Squire et al., 2013; Thompson and Bichot, 2005).

Evidence for such a saliency map is mainly provided by studies that average the activity of single neurons over multiple repetitions of the same trial condition (Armstrong et al., 2009; Bichot et al., 2001; Everling et al., 2002; Gregoriou et al., 2009; Lebedev et al., 2004; Lennert and Martinez-Trujillo, 2011; Moore and Armstrong, 2003; Rainer et al., 1998; Thompson et al., 2005a). This across-trial averaging is performed in order to overcome the substantial amount of trial-to-trial variability in the responses of single neurons (Faisal et al., 2008; Tolhurst et al., 1983; Tomko and Crapper, 1974). This method, however, may not entirely reveal the ability of the prefrontal cortex to encode attentional signals in realistic environments where the brain must direct attention on a single-trial basis despite the variability of single-neuron responses.

It is currently thought that the brain averages the activity of many neurons to overcome the variability of neuronal responses (Nienborg and Cumming, 2010; Shadlen and Newsome, 1998; Shadlen et al., 1996). To account for this, previous studies have pooled single neurons' activities recorded independently over different recording sessions into a neuronal group, sometimes referred to as a "neuronal population" (Astrand et al., 2014; Kadohisa et al., 2013; Stokes et al., 2013). This procedure assumes that single neurons fire independently from one another and that the pooled activity of individual neurons recorded during different trials approximates the activity of the neuronal population on a single trial. This assumption, however, is probably unrealistic. Single neurons in many brain areas exhibit correlated

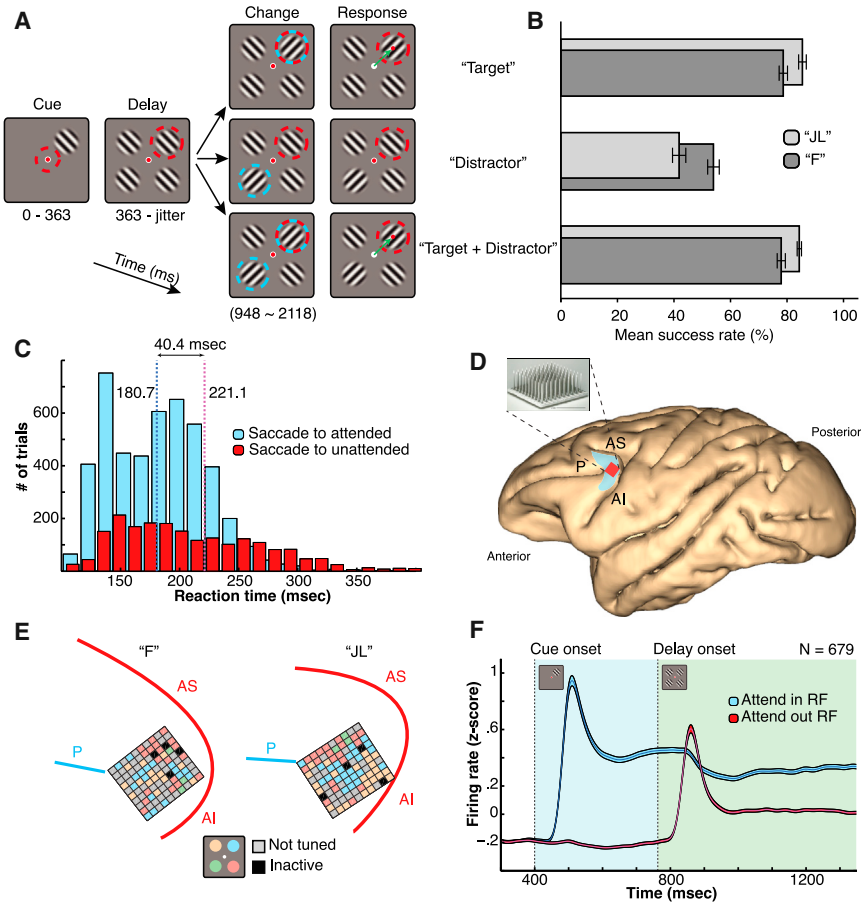

Figure 1. Behavioral Task and Electrophysiological Recordings

(A) Animals were required to saccade to the stimulus changing orientation only if that stimulus position was previously cued. Red circle: focus of attention. Blue circle: location of orientation change. Red dot: gaze position. Green arrows: saccade. Colored elements were not displayed.

(B) Behavioral performance of monkey "JL" and "F" on the three trial types. Error bars represent SEM.

(C) Reaction time distributions for saccades directed at the cued location (blue bars) compared to the uncued location (red bars). Blue and magenta lines represent the mean reaction time for saccades to the cued and uncued location, respectively (cued < uncued, $p < 0.001$, unpaired t test).

(D) Anatomical location of chronic implant. Red square represents position of multielectrode array in left hemisphere. Purple area represents roughly macaque area 8A. P: principal sulcus, AS: superior arcuate sulcus, AI: inferior arcuate sulcus.

(E) Precise location of implants in monkey "F" and "JL" according to intraoperative photography. Colors code for the spatial attention tuning of the multiunit cluster recorded at each electrode site.

(F) Normalized responses of single visually tuned neurons to a stimuli being presented inside the receptive field while attention is allocated inside (blue trace) or outside (red trace) the receptive field. Color shaded regions represent SEM.

firing (i.e., noise correlations) that can limit the efficacy of averaging and therefore affect the information content of the population (Averbeck et al., 2006a; Shadlen and Newsome, 1994). Although the precise effects of these correlations on population coding are still unclear (Ecker et al., 2011; Nienborg et al., 2012), they seem to play an important role in visual attention (Cohen and Maunsell, 2009; Mitchell et al., 2009). It has been proposed that a realistic estimate of population responses can be obtained by simultaneously recording from a group of neurons, referred to as a *neuronal ensemble* (Buzsáki, 2004; Hebb, 1949). In the primate prefrontal cortex, however, few studies have recorded from neuronal ensembles in order to understand the population dynamics underlying visual attention (Buschman and Miller, 2009; Cohen et al., 2010, 2007). Currently, whether prefrontal neuronal ensembles can encode the allocation of visual attention on a single-trial basis despite response variability and correlated firing is unclear.

To investigate this issue, we chronically implanted multielectrode arrays in area 8A of two macaque monkeys. Area 8A is a cytoarchitectonically defined granular region of the LPFC located on the prearcuate convexity, anterior to the frontal eye fields (FEF) and posterior to area 9/46 (Petrides, 2005). Neurons in this area have particularly strong attentional signals that are independent of eye movements, have attentional fields spanning both visual hemifields, and lead to specific attentional deficits when lesioned (Johnston et al., 2009; Lennert and Martinez-Trujillo, 2013; Lennert et al., 2011; Petrides, 2005). We recorded the activity of neuronal ensembles in area 8A while the animals performed a standard attentional task. From the ensemble activity, we could accurately decode the focus of attention on a single-trial basis. Additionally, we found that correlated firing between similarly tuned neurons was detrimental to the decoding of attention. Moreover, the decoding was resilient to transient distractors, predictive of behavioral outcomes, and stable across weeks of chronic recordings.

RESULTS

Neuronal Ensemble Decoding Performance

Two monkeys (*Macaca fascicularis*) performed a visual attention task while we recorded from neuronal ensembles in their left LPFC area 8A (Figure 1). The animals were instructed to covertly attend to one out of four identical Gabor stimuli, to detect a subtle change in its orientation, and to saccade to it within 400 ms of the change to obtain a juice reward (Figure 1A). The target Gabor was cued by appearing 363 ms before the other three distractors. After a variable delay period, orientation changes could happen in either the target ("Target" trials) or in the opposite distractor ("Distractor" trials). In the latter case, the monkey had to ignore the transiently changing distractor and maintain fixation

on the center dot until the end of the trial. In a third trial type, orientation changes happened simultaneously both in the target and in the opposite distractor, in which case the monkey had to saccade to the target and ignore the transient distractor ("Target + Distractor" trials). Within a given session, all three trial types were randomly interleaved, so that it was impossible for the animals to (1) predict the location of the target, (2) know whether or not a saccade would be required, and (3) know whether the change would happen in the target or in a distractor stimuli or in both.

Both monkeys performed above chance in all trial types: "Target," "Target + Distractor" (both ~80% hit rate, including fixation breaks), and "Distractor" (~60%; Figure 1B). The performance in the latter condition was lower because in some trials the monkeys made a saccade to the distractor change. Importantly, this was not due to the animals ignoring the cue and saccading to any stimulus change. In the latter scenario, the performance in the "Target + Distractor" trials would have been 50% and the performance in the "Distractor" trials would have been 0%. Further supporting that the animals allocated attention to the cued location, saccades to the distractor change had longer latencies than saccades to the target change (Figure 1C).

We recorded the activity of neuronal ensembles in area 8A of each monkey's left LPFC using a chronically implanted 96-channel multielectrode array (Figures 1D, 1E, and S1). We isolated action potentials from single neurons and multiunit clusters using standard thresholding and spike-sorting techniques (see Supplemental Experimental Procedures available online). We refer to both single units and multiunit clusters when using the general term "unit." We found units tuned for the spatial position of each one of the four possible targets, although a larger proportion of units preferred targets in the hemifield contralateral to the implant (70% contralateral versus 30% ipsilateral; Figure 1E and Supplemental Information). In agreement with previous studies (Lebedev et al., 2004; Lennert and Martinez-Trujillo, 2011, 2013), many units within the recorded ensembles showed a sustained increase in firing rate that was selective for the spatial allocation of attention to the target stimulus (Figures 1F and S2). This sustained increase in responses is a signature of visual attention at the single-cell level (Moran and Desimone, 1985; Treue and Martínez Trujillo, 1999) and corroborates that the animals attended to the target during the delay period.

The activity of each neuronal ensemble (mean [M] = 52 simultaneously recorded units, standard deviation [SD] = 7, 23 recording sessions) was inputted to a decoding algorithm capable of making single-trial predictions about both external (e.g., stimulus location) and internal (e.g., attention allocation) variables. Figure 2A depicts four example single-trial ensemble activities from the same recording session, one for each attended location. Although the exact nature of the neuronal code used by these prefrontal neuronal ensembles remains unknown, it has recently been suggested that state-of-the-art decoders such as support vector machine (SVM) (Cortes and Vapnik, 1995) might be best suited to extract the multidimensional information coded by ensembles of simultaneously recorded LPFC neurons (Astrand et al., 2014; Rigotti et al., 2013). As such, we used a SVM decoder to predict the target location during the various epochs of a trial (LIBSVM v.3.14) (Chang and Lin, 2011). Throughout the article, we refer to the cue (1), attention (2), or saccade (3) epochs and extract the corresponding single-trial average decoding accuracies. The decoder's accuracy was assessed using a standard cross-validation procedure by iteratively training the decoder on 4/5 of trials and testing its predictions in the remaining 1/5 of trials (K-fold = 5). Confusion matrices of the decoder's misclassifications were obtained to identify potential error patterns. Chance performance was determined by a permutation test that shuffles trial labels of the training set (see Supplemental Information for more details on the decoding procedure).

In order to make single-trial predictions about the cue position, the allocation of attention, and the saccade endpoint, we trained and tested the decoder at different time points during correct "Target" trials. We used different time windows to integrate the firing rate of units in the ensembles, from 20 to 800 ms. The decoder gave classification performances significantly above chance in all epochs using windows equal to or longer than 80 ms (see Figure S3). Figure 2B shows the classifier performance using two time windows, 100 (dashed red line) and 400 ms (full red line). In both scenarios the performance was significantly higher than chance (25%). For further analyses, we used the larger 400 ms window because it provided a good compromise between decoding speed and accuracy (see Figure S3).

Across all recording sessions, we found that the decoder achieved higher than chance accuracy in predicting: (1) the cue position (M = 82%, 95% confidence interval of the mean [CI] = 72%–92%, paired t test, $p < 0.001$), (2) the allocation of attention (M = 74%, CI = 65%–83%, paired t test, $p < 0.001$), and (3) the saccade endpoint (M = 98%, CI = 97%–99%, paired t test, $p < 0.001$) (Figure 2B, red line). Following cue offset, decoding accuracy reached a constant level throughout the attention epoch (~1–2 s long), a result likely attributable to the sustained activity of units encoding the attended target location (Figures 1F, 2A, and S2). These results indicate that LPFC neuronal ensembles can select a visual target among distractors within timeframes of a few hundred milliseconds.

Noise Correlations' Impact on Decoding Performance

Attention is known to have various modulatory effects on the signal-to-noise ratio of neuronal activity, including increases in firing rate (Everling et al., 2002), decreases in Fano factor (Mitchell et al., 2007), and increases in the coherence and power of local field potentials (Gregoriou et al., 2009; Womelsdorf et al., 2006). These effects have been documented using single-electrode recording methods. More recently, some studies have recorded from neuronal ensembles in the extrastriate visual area V4 and reported that attention improves performance primarily by reducing noise correlations between neurons (Cohen and Maunsell, 2009; Mitchell et al., 2009). However, whether noise correlations are always detrimental to neuronal ensemble encoding is still being debated theoretically (Ecker et al., 2011; Nienborg et al., 2012). It has recently been suggested that combining simultaneous recordings with decoding methods can reveal whether noise correlations truly limit the information coding capabilities of a neuronal population (Moreno-Bote et al., 2014).

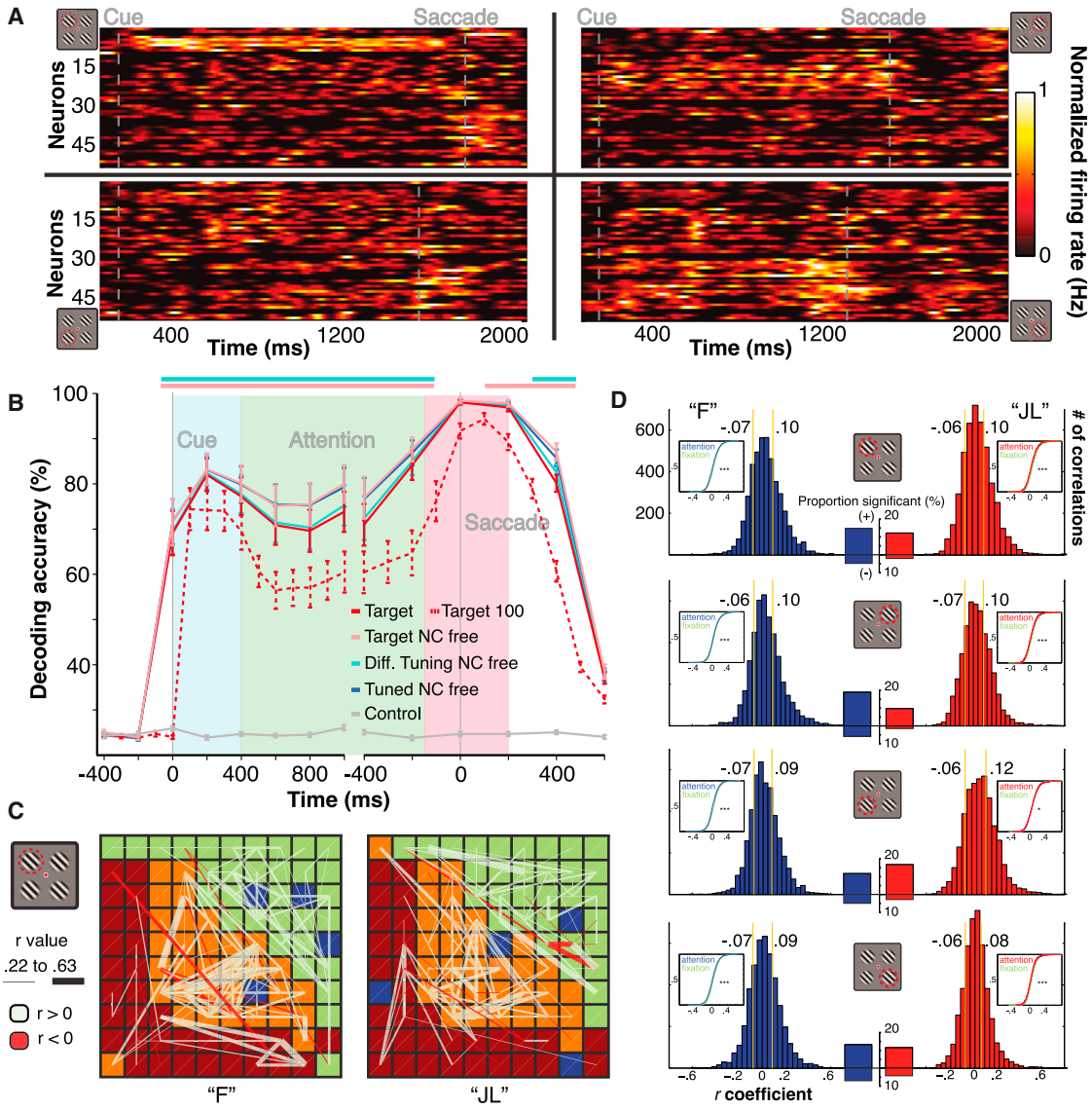

Figure 2. Neuronal Ensemble Activity and Correlated Variability

(A) Examples of four single trials of the "Target" trial type, one for each cued position. Firing rates (color scale) are normalized to maximum firing of individual units.

(B) Mean decoding accuracy pooled across sessions and monkeys for all task epochs (Cue, Attention, and Saccade). Abscissa represents the center of a 400 ms window used to train and test the decoder and the ordinate represents the decoder's performance. Target: "Target" trial type. Target 100: "Target" trial type using a 100 ms integration window. Target NC free: "Target" trial type using noise correlation free data. Diff. Tuning NC free: "Target" trials where correlations between dissimilarly tuned neurons have been selectively destroyed. Tuned NC free: "Target" trials where correlations between both similarly and dissimilarly tuned neurons have been selectively destroyed. Control: "Target" trial type using shuffled trial labels. Pink bar at the top indicates statistically significant differences between "Target" and "Target NC free" lines, and the cyan line indicates significant differences between the "Target NC free" and "Diff. Tuning NC free" lines, $p < 0.001$. There is no difference between the "Target NC free" and "Tuned NC free" lines. Error bars indicate SEM.

(C) Example noise correlation networks between units on each electrode of the array. Squares' color represents blocks of 32 electrodes.

(D) Noise correlation distributions for each attended location. Curved line plot indicate cumulative distribution functions for attention or fixation epochs. Bar graphs indicate proportion of statistically significant correlations ($p < 0.01$), positive and negative correlations kept separate. Yellow lines indicate median of positive or negative noise correlation distributions.

To investigate this issue, we quantified noise correlations between neurons in the recorded neuronal ensembles. Figure 2C illustrates correlations between simultaneously recorded units in two example sessions. Lines represent statistically significant correlations between pairs of units corresponding to different electrodes ($p < 0.05$). Most correlations were positive and small (Figure 2C; white lines). We also quantified changes in noise correlations during attentional selection of each possible target compared to a passive fixation (Figure 2D). The distribution of noise correlations between all possible pairs of units within a

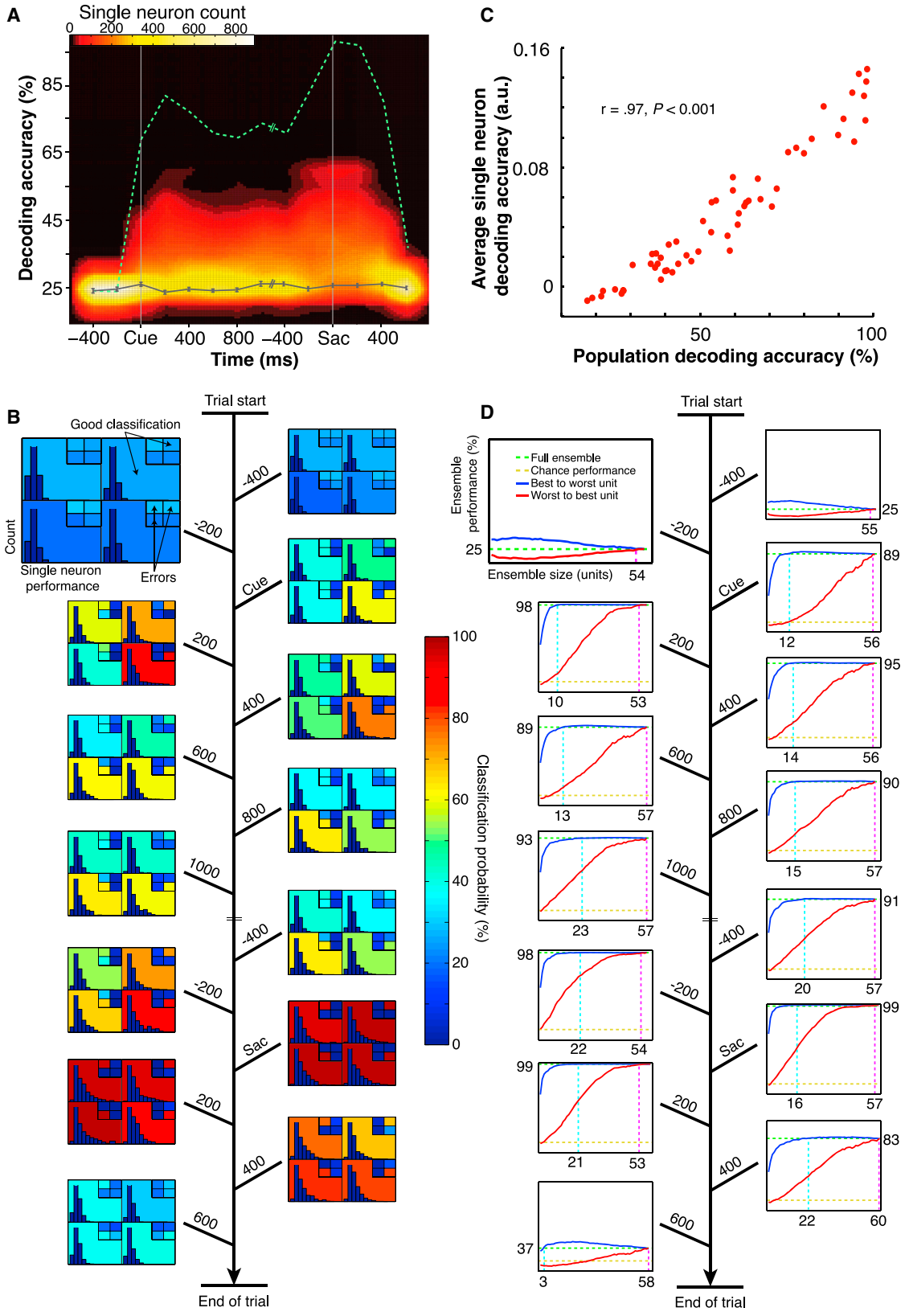

(legend on next page)

neuronal ensemble was different during attention compared to fixation ($p < 0.05$, two-sample Kolmogorov-Smirnoff test) and depended on which target attention was allocated to (Monkey "F": $p < 1 \times 10^{-10}$, Monkey "JL": $p < 1 \times 10^{-43}$, Kruskal-Wallis test).

Next, we tested the overall effects of noise correlations on neuronal ensemble coding by removing them and rerunning the previous decoding analysis. We eliminated correlations by shuffling the trials' order within each stimulus conditions separately for each unit (see Supplemental Information). This procedure destroys the temporal structure of a recording session while preserving the units' tuning and average firing rate per condition (Leavitt et al., 2013). We found that destroying all noise correlations in the recorded neuronal ensembles led to statistically significant increases in cue location (1%, CI = 0.5%–2%, paired t test, $p < 0.001$) as well as attention (6%, CI = 5%–7% = paired t test, $p < 0.001$) decoding accuracies, but we failed to find such a benefit for saccade endpoint, probably due to a ceiling effect (0.4%, CI = 0.04%–0.07%, paired t test, $p > 0.01$) (Figure 2B, pink line versus red line). These improvements were statistically greater during the attentional epoch compared to the cue epoch (6% > 1%, CI of the mean difference = 4%–6%, paired t test, $p < 0.001$), suggesting that correlations could play a different role during these two task epochs.

We further applied a shuffling procedure to selectively destroy noise correlations between dissimilarly tuned units while preserving those between similarly tuned ones (see Supplemental Information). This did not yield any change in decoding accuracy (Figure 2B, cyan line). Next, we destroyed correlations between all tuned units, which affects both correlations between dissimilarly (which have no effect) and similarly tuned units. The latter improved decoding accuracy to the same level as destroying all the correlations within the recorded population (Figure 2B, dark blue line). These results demonstrate that noise correlations have an overall modest but significant detrimental impact on the ensembles' coding of attention mainly because of correlations between similarly tuned units.

Ensemble versus Single-Neuron Decoding

Because of the neuronal heterogeneity of LPFC, some units within an ensemble may encode more information about the task than others. This leads to the question of how many neurons are required to reliably encode the different aspects of the task. Some studies have suggested that very few neurons are necessary to generate a reliable signal (Newsome et al., 1989), while other studies posit that many neurons are required (Shadlen et al., 1996). To address this issue, we first contrasted the coding performance of single units to the performance of the entire ensemble by performing a separate decoding analysis on each one of the recorded units (~1,200 data sets). As in the previous decoding analyses, the responses of each unit were inputted into the decoder and predictions were obtained and tested for all trial epochs. Figure 3A shows the decoding accuracy across all epochs for each recorded unit. While some units reached decoding accuracies up to 60% (Figure 3A; color map), none reached the average performance of the neuronal ensembles (Figure 3A; green dotted line). This analysis was replicated using a shorter time window of 100 ms; the results were similar (see Figure S4).

Next, we investigated the relationship between the performance of the ensemble and the individual performance of its single-neuron members. We addressed this question by looking at the relationship between the specific errors made when decoding from complete ensembles versus the errors made when decoding from individual units. We extracted the confusion matrices detailing the type of misclassification errors of single units and ensembles for each task epoch, and compared the two (Figures 3B and S5A, quadrants' color versus quadrants' histogram). We found that per-target ensemble decoding accuracy was strongly correlated with the average individual unit's performance within the same ensemble for the same target ($r = 0.97$, $p < 0.001$) (Figure 3C). This indicates that the ensemble performance is intrinsically tied to the properties of its individual unit members.

Finally, we asked how many units are required to reach the ensemble performance level for each individual epoch of "Target" trials (14 time points). To address this issue, we progressively added units to the decoder using two different procedures based on the units' independent classification performance: (1) from the best to the worst unit (Figure 3D, blue lines), or (2) from the worst to the best unit (Figure 3D, red lines). In the former case, a surprisingly low number of units (M = 12, SD = 7.2) was required to attain a decoding accuracy equivalent to the ensemble's performance. On the other hand, when inputting the worst units first, it generally required almost the entire population to reach the ensemble performance level (Figure 3D, pink lines). However, many more than the best units made a

Figure 3. Ensemble and Units Performance

(A) Color histogram of individual units' decoding accuracy during "Target" trials. Dotted green line and dark gray line respectively represent the neuronal ensembles average performance and the chance performance, as illustrated in Figure 2B. Abscissa represents the center of a 400 ms window used to train and test the decoder and the ordinate represents the decoder's performance.

(B) Each 2 × 2 box represents the average decoding accuracy per quadrant across ensembles in "Target" trials at different time points (monkey "F"). The histograms in each cell-quadrant represent the distribution of decoding accuracies (correct – false positives) across units for that specific quadrant. Small 2 × 2 insets within each cell represent the percentage of time that a quadrant was classified as another quadrant, as in a standard confusion matrix.

(C) Correlation between per-quadrant unit accuracy and per-quadrant ensemble accuracy for Monkey "F." Correlation coefficient for Monkey "JL" was also statistically significant ($r = 0.90$, $p < 0.001$).

(D) Each plot depicts the decoding accuracy for each task epoch (i.e., 14 time points) as units are progressively added to the ensemble for monkey "JL." The abscissa represents the number of units and the ordinate the decoding accuracy. The blue line represents accuracy when the best units are entered first in the decoder, ranked according to their individual decoding accuracy. The red line represents the opposite scenario where the worst units are entered first. The green dotted line represents the ensemble performance for the corresponding 400 ms time epoch. The yellow dotted line represents chance performance (25%). The cyan dotted line indicates the minimum number of units required to reach the average ensemble performance. The purple dotted line marks the intersection between the red line and the green dotted line.

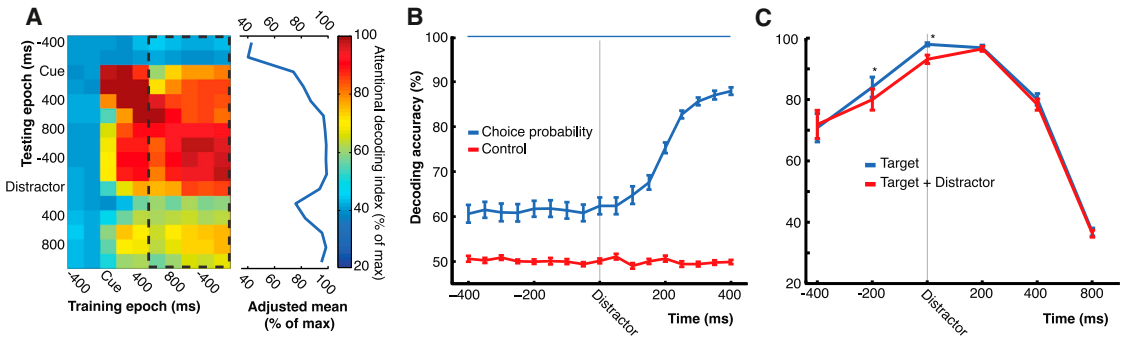

Figure 4. Distractors and Decoding Accuracy

(A) Resilience of attentional decoding during and after a salient distractor change in "Distractor" trials. Decoders were trained and tested on all possible pairs of time points. Results are expressed as percentage of maximal decoding accuracy during the attentional epoch. The focus is on decoders that were trained during the attentional epochs (black dashed rectangle). The adjusted mean from the plot on the right was computed by averaging each row inside the black rectangle. Mean is adjusted to account for the normal decay due to the time interval between training and testing epochs (see Figure S7).

(B) Population "choice probability" type analysis using the decoder to classify correct (inhibited saccade) from incorrect (saccade) trials in "Distractor" trial type. The "Control" line is obtained by shuffling trial labels. Blue line on top indicates statistically higher than chance decoding, $p < 0.001$. Of interest, error prediction is possible even before the onset of the distractor event.

(C) Effect of a salient distractor change when synchronous with a change in the attended target. *: statistically significant differences, $p < 0.001$. Errors bars represent SEM in (B) and (C).

significant contribution to the ensemble performance (Figure 3D, red lines departing from yellow "chance" lines). This suggests that although decoding performance is most influenced by the best-tuned units in the ensemble, most units can contribute to the ensemble code.

Overall, these results indicate that the information contained in the firing of an ensemble of simultaneously recorded LPFC units is significantly higher than the one contained in the firing of the best-tuned single unit. Importantly, the information contained in the firing of a dozen of well-tuned neurons matches the one of a population of approximately 50 units.

Distractor Interference of Ensemble Activity

Relative to other brain areas, the firing of single neurons in LPFC is robust to distractor interference occurring outside of the focus of attention (Noudoost et al., 2010; Suzuki and Gottlieb, 2013). How ensembles of correlated neurons react to distractors, however, remains poorly documented. To assess the robustness of the neuronal ensemble code to salient distractors, we included in our task two types of trials involving distractor changes (see Figure 1A; "Distractor" and "Target + Distractor" trials).

In "Distractor" trials, the monkeys had to inhibit saccading to the orientation change in the distractor and had to maintain gaze on the fixation point in order to receive a reward. Because of the high saliency of the change, the animals saccaded to the distractor in a proportion of trials, which decreased behavioral performance by ~30% compared to "Target" trials (Figure 1B). We examined the neuronal ensembles' coding during the attention epoch for correlates of this interference. Since in these trials the distractor change always occurred opposite to the target, visual responses to the distractor could inform the decoder about the allocation of attention, precluding using the previous analysis strategy to quantify the interference (see Figure S6 for an example of the bias). Thus, in order to control for this bias, we trained the decoder during the attentional epoch before the distractor change onset to obtain a baseline attentional code and predicted the target location during and after the distractor change using this code. Because the decoding accuracy decays as a function of the time difference between training and testing time point (−2% per 100 ms; Figure S7), we adjusted the results to take this effect into account (see Supplemental Information).

We found that the distractor change elicited a drop in decoding accuracy of approximately 25% compared to maximum accuracy (Figure 4A). Importantly, this interference was observed during correct trials—i.e., trials where the monkeys were able to withhold saccading to the distractor change. Coherently with behavioral outcome, the interference was only transient and the decoding accuracy rapidly increased back to predistractor baseline levels (Figure 4A). These results indicate that the activity of LPFC neuronal ensembles was initially perturbed by a salient distractor change and that when the animals successfully inhibited saccading to the distractor, ensemble activity promptly recovered to predistractor levels.

Next, we contrasted the neuronal ensemble's activity in successful "Distractor" trials with the ensemble's activity in error trials where the animals saccaded to the distractor change. To do so, we used the decoder to discriminate correct trials from errors using the ensemble's activity before, during, and after the distractor change, as in a traditional "choice probability" analysis (Britten et al., 1996). We found that postdistractor change ensemble activity was highly predictive of errors (~88%, paired t test, $p < 0.001$, Figure 4B). Importantly, predistractor neuronal ensemble activity was predictive of the animals' ability to inhibit saccading to the upcoming distractor change. (Decoder performance = ~60%, chance performance = ~50%, paired t test, $p < 0.001$, Figure 4B.) These results suggest that the susceptibility of the animal to distraction can be predicted from LPFC neuronal ensemble activity even before the onset of the distracting event.

Finally, we analyzed trials where the distractor change occurred simultaneously with a change in the target (Figure 1A;

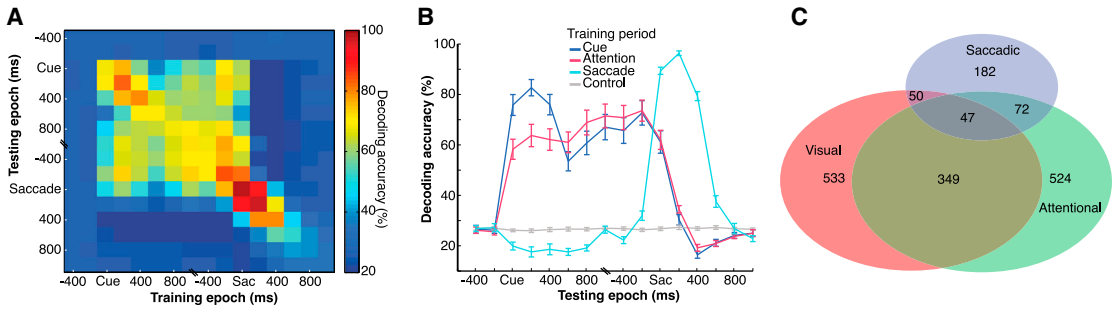

Figure 5. Decoding of Attention and Saccades

(A) Generalizability of the neuronal ensemble activity across all epochs of "Target" trials. The decoder is trained and tested on all possible pairs of time points. Color of each square represents the decoding accuracy of a decoder trained and tested on the corresponding time points.

(B) Quantitative representation of across-epochs generalizability of the decoder. Cue, Attention, and Saccade lines represent column Cue+200, 800, and Saccade +200 in Figure 5A. Control line corresponds to column Cue-400. Error bars indicate SEM.

(C) Venn diagram representing the absolute number of units belonging to each of three tuning categories (visual, attentional, and saccadic). Intersections represent neurons that belong to more than one category.

"Target + Distractor"). At a behavioral level, this simultaneous distractor change had almost no effect on the monkeys performance relative to when the target change occurred alone (mean difference between "Target" and "Target + Distractor" trial types = 0.9%, CI = −0.8%–2.6%, paired t test, p = 0.3, see Figure 1B). We contrasted the neuronal ensemble's activities during both of these trial types by training the decoder during "Target" trials and predicting the target position during "Target + Distractor" trials. Correspondingly, we found that the neuronal ensemble's activity was only slightly affected by the presence of the distractor change (mean difference between "Target" and "Target + Distractor" decoding = 4.5%, CI = 2.6–6.3, p < 0.001, paired t test, Figure 4C). Thus, both the encoding of the allocation of attention by LPFC neuronal ensembles and the behavioral performance of the animals were relatively robust to distractor changes concurring with target changes. This is very different from the effects of isolated distractor changes, suggesting that a highly salient event occurring at the attended location overrides or masks (physiologically and behaviorally) the saliency of distractor events occurring at unattended locations.

Ensemble Codes for Attentional Selection and Saccades

It has been suggested that oculomotor mechanisms play a critical role in the deployment of visual attention (Rizzolatti et al., 1987). Some microstimulation and pharmacological studies have supported this idea by showing that these two processes are mediated by the same neuronal populations in prefrontal cortex (Moore and Armstrong, 2003; Müller et al., 2005; Wardak et al., 2006). However, other studies have argued that different neuronal types within these populations make different contributions to attentional selection and eye movements (Gregoriou et al., 2012; Thompson et al., 2005b). Assessing the similarity of the neuronal ensemble codes for attention and saccade might provide some insight on this controversy.

We reasoned that if the ensemble code for attention and saccade is the same, then a decoder trained during the attentional epoch should make accurate predictions about the saccade endpoint, and vice versa. Thus, we trained the decoder during "Target" trials at several time points and tested its decoding performance across all other time points, generating a training epoch by testing epoch matrix of decoding accuracies (Figure 5A). Patterns of good generalizability across task epochs appear in Figure 5A as rectangular areas of high decoding accuracy. We found that (1) training the decoder during the cue or the attention epoch yields high classification accuracy when testing during either of these two epochs, but low accuracy when testing during the saccade epoch, and (2) that training the decoder during the saccade epoch yields high decoding accuracy when testing during the same epoch, but low accuracy when testing during either the cue or the attention epoch. We quantified these observations in Figure 5B by contrasting the performance of three decoders, one trained on each epoch. Clearly, the performance of the decoders trained during the visual and attention epoch was very similar, but both failed to make accurate predictions during the saccade epoch. These results confirm the prediction that the neuronal ensemble's activity patterns corresponding to visual/attentional and saccadic signals differ substantially. This can either suggest that different neurons within the ensembles underlie attentional selection and saccades or that the same neurons encode both throughout the trial, although in a different format. In favor of the former interpretation, we found that a high proportion of attentional neurons share similar visual tuning properties (349/524; 65%, Figure 5C), while few of these neurons carry any information about the saccade (72/524; 14%).

Decoding Accuracy of Sorted versus Thresholded Activity

The field of neural prosthetics seeks to bridge the brain to the world by using brain signals to control objects in the environment (e.g., artificial limbs, computers, etc.) (Andersen et al., 2010; Donoghue, 2008). These brain-machine interfaces require the real-time processing of neuronal ensemble signals to feed control signals to the prosthetics within a timeframe compatible with behavior. Sorting spikes is a time-consuming and computationally demanding operation that can hinder real-time processing. Therefore, alternative methods must be considered to avoid this operation. It has been proposed that voltage-thresholded

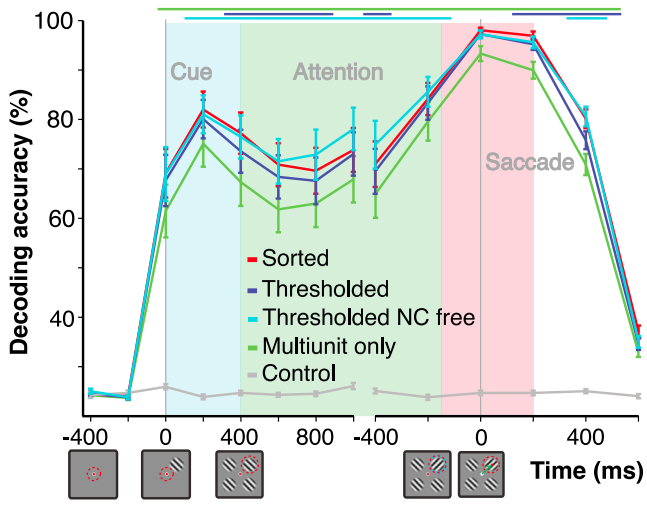

Figure 6. Spike-Sorted versus Thresholded Ensemble Activity

Neuronal ensemble decoding accuracy for all epochs of "Target" trials, using either spike-sorted ("Sorted" line) or thresholded data ("Tresholded" line). Blue bar on top of plot indicates time points of significant differences between "Sorted" and "Thresholded" data ($p < 0.001$, paired t test). The cyan line indicates the decoding performance of thresholded data with intrinsic noise correlations destroyed (Thresholded NC free). Cyan bar on top indicates points of significant differences between "Thresholded" and "Thresholded NC free" data ($p < 0.001$, paired t test). "Multiunit only" corresponds to a data set which includes multiunit clusters but excludes all isolated single units. Green bar on top indicates the epochs for which "Multiunit only" decoding is statistically inferior to "Sorted" decoding accuracy ($p < 0.001$, paired t test). Error bars indicate SEM.

unsorted activity in motor or premotor areas carries sufficient information to reliably guide a brain-machine interface, removing the need to sort spikes (Chestek et al., 2011; Fraser et al., 2009). Thus, we tested whether in our experiment decoding from fully spike-sorted neuronal ensembles yields similar performance as decoding from neuronal activity extracted using a fast and simple voltage thresholding operation.

We extracted the thresholded activity by applying a voltage threshold to the raw high-frequency voltage traces (see Supplemental Information). This operation puts together all single- and multiunit activity recorded at a given electrode site, yielding a single multiunit cluster per electrode. We then compared the decoding accuracy using thresholded signals to the accuracy using spike-sorted signals. We found that decoding the cue, attended location, and saccade endpoint using the thresholded data yielded slightly lower but comparable performance to the original sorted signal (Figure 6, red line versus blue line, cue = −2%, attention = −2%, saccade, = −0.4%, paired t test, $p < 0.001$). This indicates that the pooled activity of units surrounding a recording electrode in LPFC carries a similar amount of information as the sorted activity of single units. Remarkably, eliminating noise correlations between electrode clusters in the thresholded data yielded an increase in decoding accuracy, as observed with the spike-sorted data set (Figure 6, cyan line versus blue line, paired t test, $p < 0.001$).

To further examine the contribution of well-isolated single units and multiunit clusters to the decoding accuracy of the thresholded data, we re-sorted our data set to exclude all single units from the recordings. We found that decoding from multiunits only yielded above-chance decoding accuracy, although not to the level obtained by including single units to the data set (Figure 6, green line versus blue line, paired t test, $p < 0.001$). This indicates that multiunit clusters contain an important amount of information about the task; however, single units significantly add to that information.

Stability of Neuronal Ensemble Coding over Time

Microcircuits within the LPFC are known to be very plastic, dynamically adapting as a function of the task at hand (Buschman et al., 2012; Mante et al., 2013; Miller and Cohen, 2001). However, some applications such as chronic neural prosthetics require a stable neuronal code in order to accurately decode the subject's intentions for a prolonged period of time. We asked whether the neuronal ensemble code underlying attentional selection of visual targets could be stable over long time periods. We had the opportunity to investigate this issue because our recordings extended over multiple weeks using the same chronic multielectrode implants in the same animals. To address this question, we trained a decoder on the attentional epoch of a specific session and used it to predict attention allocation in other recording sessions. We replicated this procedure for every possible pairs of recording sessions, from training and testing on the same session to training and testing on sessions that occurred more than a month apart. Importantly, as in the previous analysis, we used only unsorted thresholded data (i.e., one multiunit cluster per electrode) and the same electrodes across all sessions (see Supplemental Information).

We generated a matrix of training by testing session illustrating the generalizability of the attentional code as a function of time. The matrix shows that a decoder trained on day 1 can make accurate predictions even a month later, suggesting a high generalizability of the attentional code across sessions recorded on different days (Figure 7A). We have replicated this analysis for the visual and saccade epoch and found a comparable generalizability (Figures 7B and 7C). For control purposes, we tested the decoder on a different set of adjacent electrodes within the same brain area (Figures 7A–7C; con 1 & con 2). In this case, decoding accuracy dropped to chance, indicating that although the neuronal code is stable over time within a given ensemble, it does not generalize to nearby neuronal ensembles.

One likely explanation for the stability of the decoder over time is that the neuronal activity recorded from each electrode preserves its tuning despite possible changes in the units' isolation across sessions (e.g., loss of units and emergence of new units due to the slight movement of the electrodes inside the cortex). To test this hypothesis we examined the tuning of multiunit activity corresponding to each one of the different electrodes across sessions. Figure 7D depicts four example multiunit clusters tuned for each of the four attended locations. Despite modest changes in absolute firing rates over time, the tuning of each unit seemed very stable over a time span of more than a month. We further quantified this observation by computing the standard deviation of the spatial tuning of the example units in a two-dimensional space. We found that despite small variations in absolute firing rate (mean SD of Euclidian distances = 8.6),

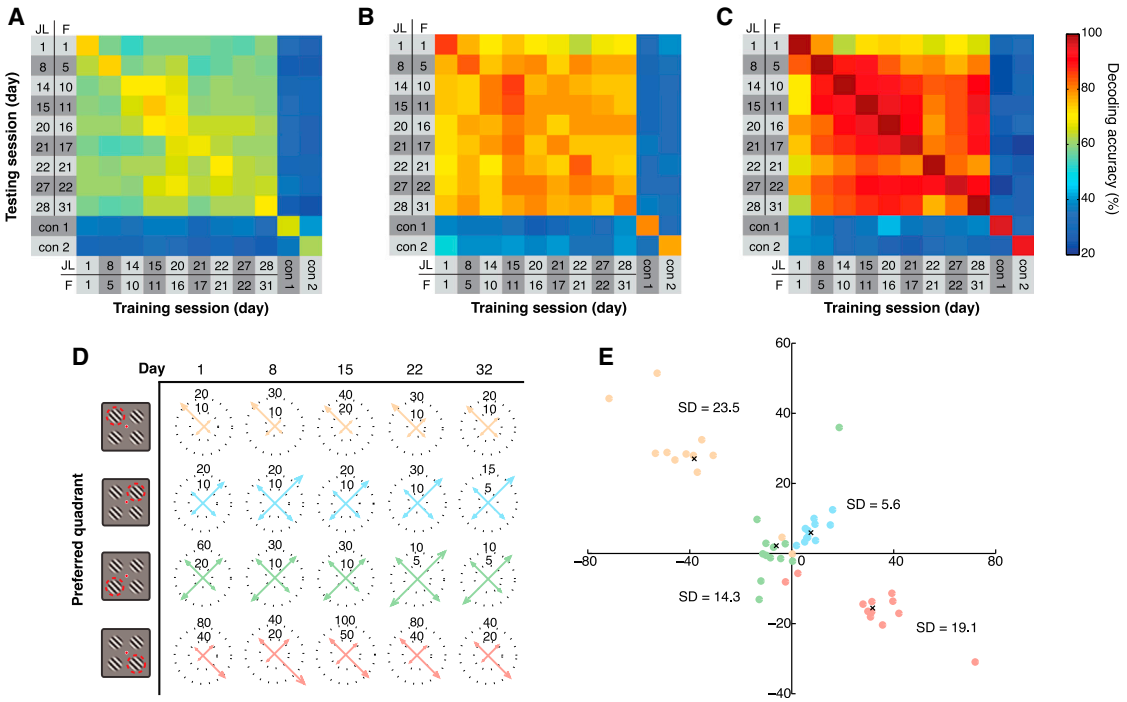

Figure 7. Coding Stability of Neuronal Ensemble across Recording Sessions

(A) Generalizability of decoders trained during the attention epoch across recording sessions (days). The decoder was trained and tested on every pair of sessions within the attention epoch. Squares' color represents decoding accuracy, pooled across monkeys. "con 1" and "con 2" are control sessions recorded from adjacent blocks of electrodes within the same cortical region.

(B) Same as in (A), but for the Cue epoch.

(C) Same as in (A), but for the Saccade epoch.

(D) Average firing rates during the attentional epoch are depicted for four example multiunit clusters, each with a different attentional field, over the course of five weeks of recording.

(E) Each dot represents the sum of vectors defined by the firing rate of a unit to the four possible attended locations over the course of one session. Each color represents a different unit, as in (D). Each dot represents a different session for that unit. The "x" marks represent the centroid of mass of each unit cluster. The standard deviation of Euclidian distances between each dot and its associated centroid was computed to quantify the tuning similarity over time independently for each unit.

relative tuning was mainly preserved across sessions (mean r of clusters distribution = 0.46) (Figure 7E). Thus, although different single units might have contributed to the spikes recorded on a given electrode from day to day (Dickey et al., 2009), the multiunit activity remained relatively stable over time. This could explain why the neuronal ensemble codes underlying visual, attentional, and saccadic signals were found to be stable over multiple weeks.

DISCUSSION

Coding of Attention by LPFC Ensembles

The orienting of attention is a dynamic process unfolding over a subsecond timescale (Posner, 1980). However, most neural correlates of visual attention in the prefrontal cortex of nonhuman primates have been obtained by pooling the activity of single neurons over a series of trials (Armstrong et al., 2009; Bichot et al., 2001; Everling et al., 2002; Gregoriou et al., 2009; Lebedev et al., 2004; Lennert and Martinez-Trujillo, 2011; Moore and Armstrong, 2003; Rainer et al., 1998; Thompson et al., 2005a). Although these studies have helped establish a link between attention and single-neuron responses, to be ecologically valid, neural correlates of attention should be derived from single-trial measurements.

Our results show that a machine-learning algorithm using the activity of neuronal ensembles in area 8A can decode the allocation of attention on a single-trial basis and over time windows as low as 100 ms. This result supports the role of LPFC in top-down visual attention by showing that attentional signals originating from this region could modulate visual activity on a timescale coherent with behavior, despite the variability in single-neuron responses (Desimone and Duncan, 1995; Squire et al., 2013). This result agrees with a study showing that the focus of spatial attention can be tracked from the activity of single neurons in the LPFC of macaques (Buschman and Miller, 2009).

Another constraint on neuronal ensemble computations is due to correlated trial-to-trial variability between single neurons (Cohen and Maunsell, 2009; Mitchell et al., 2009). It has been proposed that noise correlations can limit the amount of information carried by a neuronal ensemble (Shadlen et al., 1996). However, others have argued that, under certain circumstances, noise correlations may be beneficial to ensemble

coding, particularly when they occur between neurons with different tuning properties (Averbeck et al., 2006a). We showed that removing the entire intrinsic noise correlation structure of the neuronal ensembles increases decoding accuracy of attention by a small but significant amount. This effect was mainly due to removing correlations between similarly tuned neurons, which is in agreement with theoretical models (Averbeck et al., 2006b; Moreno-Bote et al., 2014). Destroying correlations between dissimilarly tuned neurons did not lead to significant changes in decoding accuracy. This may be explained by the fact that, in our data set, these correlations were usually small in number and amplitude. Overall, these observations agree with studies demonstrating that visual attention improves behavioral performance by decreasing noise correlations in visual cortical neurons (Cohen and Maunsell, 2009; Mitchell et al., 2009).

An implication of the previous results pertains to the inferences made from pooling nonsimultaneously recorded single neurons into a "neuronal population." Since this method cannot capture correlated variability between units, it assumes that neurons make independent contribution to the information content of the population activity. Our results indicate that such a method leads to a modest yet significant overestimation of the encoding efficiency. Thus, measurements of neuronal ensembles activity yield more realistic estimates of the computational power of neuronal populations.

One issue that has been matter of debate is whether the performance of single neurons is comparable to the one of neuronal populations (Newsome et al., 1989; Rochel and Cohen, 2007; Sanger, 2003). We found that although the best single units could inform about the allocation of attention, neuronal ensembles always performed significantly better. Surprisingly, a small ensemble composed of the best 12 units could reproduce the decoding accuracy of an entire ensemble of ~50 units. This suggests that a downstream neuron may only "read out" from a small group of informative units to encode the allocation of attention, minimizing metabolic and wiring costs (Laughlin and Sejnowski, 2003; Niven and Laughlin, 2008). Interestingly, when inputting the worst units first into the iterative decoder of Figure 3D, we found that most units carried information about the allocation of attention. One possible explanation for these observations is that less informative neurons contribute differently to the network computation (e.g., normalization, noise reduction, etc.). It may be that the most informative neurons reflect the output of the computation rather than its intermediate steps. Layer-specific recordings would help answer this question (Hampson et al., 2012).

Responses of LPFC Ensembles to Distractors

Single neurons encoding the allocation of attention in prefrontal cortex are less sensitive to distracting stimuli relative to other brain areas (Noudoost et al., 2010; Suzuki and Gottlieb, 2013). However, how ensembles of LPFC neurons react to distractors on a single-trial basis has not been explored. In the current study, we showed that the behavioral suppression of a distractor was associated with a mild, temporary interference of neuronal ensemble coding. For a few milliseconds after the distractor change, decoding accuracy decreased by ~25%. This interference was likely caused by a transient burst of activity from units with the distractor change inside their receptive field (Figure S6A). In correct trials, this transient activity could also result from a rapid switch of the focus of attention toward the salient distractor followed by a quick switch back to the target (Busse et al., 2008).

This interpretation can be related to the lack of interference in trials where distractor and target changes concurred ("Target + Distractor"). Here, exogenous attention was likely not allocated to the distractor but remained on the endogenously attended target. This result agrees with a previous report of endogenous dominating over exogenous attention at high stages of visual processing (Hopfinger and West, 2006). Importantly, the extent of changes in the ensemble coding accuracy was linked to the animals' behavioral performance. When analyzing this neural-behavioral relationship on a single-trial basis, we found that trial-to-trial variations in the neuronal ensemble activity pattern could predict behavioral susceptibility to the distractor change (Cohen and Maunsell, 2010). This prediction could be done even a few hundred milliseconds before the onset of the distracting event, suggesting that the quality of attentional filtering is reflected in the neuronal ensemble activity.

Coding of Attention and Saccades by LPFC Ensembles

Eye movements orient the retinas toward events that are behaviorally relevant in the environment, reflecting a close relationship between attention and saccades (Deubel and Schneider, 1996; Moore et al., 2003; Rizzolatti et al., 1987). However, during covert (Posner et al., 1982) and divided attention (Niebergall et al., 2011) tasks, the allocation of attention can be dissociated from saccades, suggesting that these two processes might be subserved by distinct, but related, neuronal subpopulations (Gregoriou et al., 2012; Pouget et al., 2009; Thompson et al., 2005b). Here we showed that distinct ensemble activity patterns signal the allocation of attention and saccade endpoint, providing evidence that these two processes are dissociable at the level of ensembles. Our results agree with previous studies in area 8A that dissociate the allocation of spatial attention from saccade goal (Everling et al., 2002; Lebedev et al., 2004; Lennert and Martinez-Trujillo, 2011, 2013). Visual-attentional and saccade neurons may make different contributions to one or the other process, implementing a transformation from a visual saliency map to an oculomotor map within the LPFC (Takeda and Funahashi, 2002). It is also possible that the same neurons carry different information throughout a trial, dynamically changing from attentional to saccade coding. This dynamic coding has been well documented in populations of prefrontal neurons (Stokes et al., 2013). This interpretation would entail that the same neurons carry information about both attention and saccade. However, when examining the tuning of attentional neurons during the saccade epoch, 76% of them do not carry information about the saccade endpoint. In contrast, 65% of attentional neurons carried information about the cue position. Interestingly, only 26% of all task-tuned neurons contained any information about saccade endpoint. This is in contrast with the FEF, where ~60% of tuned neurons exhibit movement activity (Bruce and Goldberg, 1985). This observation could be explained by a rostral-caudal model of frontal hierarchical

organization, whereby caudal areas are relatively more involved in the motor transformation than in the cognitive control process (Badre and D'Esposito, 2009; Petrides, 2005).

Relevance to Cognitive Neural Prosthetics

It has been suggested that decisions, forward estimations, and even learning-related neural signals could be decoded to control a brain-machine interface that would produce behavioral outcomes according to a subject's intentions and motivations (Andersen et al., 2010; Musallam et al., 2004). Our results support this proposal. We found that the focus of attention could be quickly (within 100–400 ms) and reliably decoded using chronic multielectrode array recordings from LPFC and a simple voltage-threshold operation. Moreover, we showed that multiunit activity that excludes spikes from well-isolated single neurons carries sufficient information to accurately decode the allocation of attention. This result is encouraging for neural prosthetic applications using similar chronic implants, which tend to lose single unit isolation over time (Chestek et al., 2011).

From a physiological standpoint, it is surprising that losing this single-cell resolution does not dramatically alter the information content of recorded signals. One possible explanation for this result is that the neurons contributing to the signals captured by a given electrode are located within the same cortical column and share similar tuning properties (Constantinidis et al., 2001; Opris et al., 2012). This topographic organization of area 8A and its location on the cortical surface make it a potential target for chronic multielectrode array implants to provide signals for cognitive brain-machine interfaces. Further supporting this idea, the decoding of attentional allocation using LPFC neural ensemble activity was stable over multiple weeks of recording. The upper limit of this stability was not investigated in the current experiment; thus, it is plausible that accurate predictions could have been made for longer since the generalizability of the decoder did not seem to decay over time.

Previous studies have suggested that the microcircuits within LPFC are very plastic, or dynamically changing as a function of training during a given task (Buschman et al., 2012; Mante et al., 2013; Miller and Cohen, 2001). Our results further suggest that, despite such plasticity, visual, attentional, and saccadic representations are encoded within a map that remains stable over time. It has also been indicated that multielectrode arrays may slightly change position in the cortex and thus pick up signals from different neurons over long intervals of time (Dickey et al., 2009). Surprisingly, this variability did not seem to affect the decoder. In conclusion, our findings demonstrate the capacity of area 8A neuronal ensembles to filter visual information within an ecologically valid timeframe and encourage the use of neural signals from this area for cognitive neural prosthetic applications.

EXPERIMENTAL PROCEDURES

Experiments complied with the Canadian Council of Animal Care guidelines and were approved by the McGill Animal Care Committee. Monkeys performed a visual selective attention task. A trial started when the monkey directed its gaze on a fixation spot and pressed a lever. Following the onset of a cue grating stimulus, the monkey allocated attention to the cued stimulus while maintaining his gaze on the fixation point. The monkey had to saccade to the target upon a change in its orientation and ignore changes in distractor stimuli to obtain a juice reward. Action potentials from ensembles of neurons were recorded using a chronically implanted multielectrode array. Neuronal ensemble activity was decoded using a support vector machine to predict the allocation of attention on a single-trial basis.

SUPPLEMENTAL INFORMATION

Supplemental Information includes seven figures and Supplemental Experimental Procedures and can be found with this article online at http://dx.doi.org/10.1016/j.neuron.2014.11.021.

ACKNOWLEDGMENTS

This work was supported by grants to J.M.-T. from the CIHR, NSERC, EJLB Foundation, and Canada Research Chair program. The NSERC Alexander Graham Bell Canada Graduate Scholarship supported S.T. We thank Mr. Walter Kucharski, Mr. Stephen Nuara, and Mr. Rishi Rajalingham for technical support. We also thank the members of the M.-T. lab for useful comments on previous versions of this manuscript.

Accepted: November 13, 2014
Published: December 11, 2014

REFERENCES

Andersen, R.A., Hwang, E.J., and Mulliken, G.H. (2010). Cognitive neural prosthetics. Annu. Rev. Psychol. *61*, 169–90–C1–3.

Armstrong, K.M., Chang, M.H., and Moore, T. (2009). Selection and maintenance of spatial information by frontal eye field neurons. J. Neurosci. *29*, 15621–15629.

Astrand, E., Enel, P., Ibos, G., Dominey, P.F., Baraduc, P., and Ben Hamed, S. (2014). Comparison of classifiers for decoding sensory and cognitive information from prefrontal neuronal populations. PLoS ONE *9*, e86314.

Averbeck, B.B., Latham, P.E., and Pouget, A. (2006a). Neural correlations, population coding and computation. Nat. Rev. Neurosci. *7*, 358–366.

Averbeck, B.B., Sohn, J.-W., and Lee, D. (2006b). Activity in prefrontal cortex during dynamic selection of action sequences. Nat. Neurosci. *9*, 276–282.

Badre, D., and D'Esposito, M. (2009). Is the rostro-caudal axis of the frontal lobe hierarchical? Nat. Rev. Neurosci. *10*, 659–669.

Bichot, N.P., Thompson, K.G., Chenchal Rao, S., and Schall, J.D. (2001). Reliability of macaque frontal eye field neurons signaling saccade targets during visual search. J. Neurosci. *21*, 713–725.

Britten, K.H., Newsome, W.T., Shadlen, M.N., Celebrini, S., and Movshon, J.A. (1996). A relationship between behavioral choice and the visual responses of neurons in macaque MT. Vis. Neurosci. *13*, 87–100.

Bruce, C.J., and Goldberg, M.E. (1985). Primate frontal eye fields. I. Single neurons discharging before saccades. J. Neurophysiol. *53*, 603–635.

Buschman, T.J., and Miller, E.K. (2007). Top-down versus bottom-up control of attention in the prefrontal and posterior parietal cortices. Science *315*, 1860–1862.

Buschman, T.J., and Miller, E.K. (2009). Serial, covert shifts of attention during visual search are reflected by the frontal eye fields and correlated with population oscillations. Neuron *63*, 386–396.

Buschman, T.J., Denovellis, E.L., Diogo, C., Bullock, D., and Miller, E.K. (2012). Synchronous oscillatory neural ensembles for rules in the prefrontal cortex. Neuron *76*, 838–846.

Busse, L., Katzner, S., and Treue, S. (2008). Temporal dynamics of neuronal modulation during exogenous and endogenous shifts of visual attention in macaque area MT. Proc. Natl. Acad. Sci. USA *105*, 16380–16385.

Buzsáki, G. (2004). Large-scale recording of neuronal ensembles. Nat. Neurosci. *7*, 446–451.

Chang, C.-C., and Lin, C.-J. (2011). LIBSVM: A Library for Support Vector Machines. ACM Transactions on Intelligent Systems and Technology *2*.

Chestek, C.A., Gilja, V., Nuyujukian, P., Foster, J.D., Fan, J.M., Kaufman, M.T., Churchland, M.M., Rivera-Alvidrez, Z., Cunningham, J.P., Ryu, S.I., and Shenoy, K.V. (2011). Long-term stability of neural prosthetic control signals from silicon cortical arrays in rhesus macaque motor cortex. J. Neural Eng. *8*, 045005.

Cohen, M.R., and Maunsell, J.H.R. (2009). Attention improves performance primarily by reducing interneuronal correlations. Nat. Neurosci. *12*, 1594–1600.

Cohen, M.R., and Maunsell, J.H.R. (2010). A neuronal population measure of attention predicts behavioral performance on individual trials. J. Neurosci. *30*, 15241–15253.

Cohen, J.Y., Pouget, P., Woodman, G.F., Subraveti, C.R., Schall, J.D., and Rossi, A.F. (2007). Difficulty of visual search modulates neuronal interactions and response variability in the frontal eye field. J. Neurophysiol. *98*, 2580–2587.

Cohen, J.Y., Crowder, E.A., Heitz, R.P., Subraveti, C.R., Thompson, K.G., Woodman, G.F., and Schall, J.D. (2010). Cooperation and competition among frontal eye field neurons during visual target selection. J. Neurosci. *30*, 3227–3238.

Constantinidis, C., Franowicz, M.N., and Goldman-Rakic, P.S. (2001). Coding specificity in cortical microcircuits: a multiple-electrode analysis of primate prefrontal cortex. J. Neurosci. *21*, 3646–3655.

Cortes, C., and Vapnik, V. (1995). Support-vector networks. Mach. Learn. *20*, 273–297.

Desimone, R., and Duncan, J. (1995). Neural mechanisms of selective visual attention. Annu. Rev. Neurosci. *18*, 193–222.

Deubel, H., and Schneider, W.X. (1996). Saccade target selection and object recognition: evidence for a common attentional mechanism. Vision Res. *36*, 1827–1837.

Dickey, A.S., Suminski, A., Amit, Y., and Hatsopoulos, N.G. (2009). Single-unit stability using chronically implanted multielectrode arrays. J. Neurophysiol. *102*, 1331–1339.

Donoghue, J.P. (2008). Bridging the brain to the world: a perspective on neural interface systems. Neuron *60*, 511–521.

Ecker, A.S., Berens, P., Tolias, A.S., and Bethge, M. (2011). The effect of noise correlations in populations of diversely tuned neurons. J. Neurosci. *31*, 14272–14283.

Everling, S., Tinsley, C.J., Gaffan, D., and Duncan, J. (2002). Filtering of neural signals by focused attention in the monkey prefrontal cortex. Nat. Neurosci. *5*, 671–676.

Faisal, A.A., Selen, L.P.J., and Wolpert, D.M. (2008). Noise in the nervous system. Nat. Rev. Neurosci. *9*, 292–303.

Fraser, G.W., Chase, S.M., Whitford, A., and Schwartz, A.B. (2009). Control of a brain-computer interface without spike sorting. J. Neural Eng. *6*, 055004.

Gregoriou, G.G., Gotts, S.J., Zhou, H., and Desimone, R. (2009). High-frequency, long-range coupling between prefrontal and visual cortex during attention. Science *324*, 1207–1210.

Gregoriou, G.G., Gotts, S.J., and Desimone, R. (2012). Cell-type-specific synchronization of neural activity in FEF with V4 during attention. Neuron *73*, 581–594.

Hampson, R.E., Gerhardt, G.A., Marmarelis, V., Song, D., Opris, I., Santos, L., Berger, T.W., and Deadwyler, S.A. (2012). Facilitation and restoration of cognitive function in primate prefrontal cortex by a neuroprosthesis that utilizes minicolumn-specific neural firing. J. Neural Eng. *9*, 056012.

Hebb, D.O. (1949). The Organization of Behavior. (New York: Wiley & Sons).

Hopfinger, J.B., and West, V.M. (2006). Interactions between endogenous and exogenous attention on cortical visual processing. Neuroimage *31*, 774–789.

Johnston, K., DeSouza, J.F.X., and Everling, S. (2009). Monkey prefrontal cortical pyramidal and putative interneurons exhibit differential patterns of activity between prosaccade and antisaccade tasks. J. Neurosci. *29*, 5516–5524.

Kadohisa, M., Petrov, P., Stokes, M., Sigala, N., Buckley, M., Gaffan, D., Kusunoki, M., and Duncan, J. (2013). Dynamic construction of a coherent attentional state in a prefrontal cell population. Neuron *80*, 235–246.

Katsuki, F., and Constantinidis, C. (2012). Early involvement of prefrontal cortex in visual bottom-up attention. Nat. Neurosci. *15*, 1160–1166.

Laughlin, S.B., and Sejnowski, T.J. (2003). Communication in neuronal networks. Science *301*, 1870–1874.

Leavitt, M.L., Pieper, F., Sachs, A., Joober, R., and Martinez-Trujillo, J.C. (2013). Structure of spike count correlations reveals functional interactions between neurons in dorsolateral prefrontal cortex area 8a of behaving primates. PLoS ONE *8*, e61503.

Lebedev, M.A., Messinger, A., Kralik, J.D., and Wise, S.P. (2004). Representation of attended versus remembered locations in prefrontal cortex. PLoS Biol. *2*, e365.

Lennert, T., and Martinez-Trujillo, J. (2011). Strength of response suppression to distracter stimuli determines attentional-filtering performance in primate prefrontal neurons. Neuron *70*, 141–152.

Lennert, T., and Martinez-Trujillo, J.C. (2013). Prefrontal neurons of opposite spatial preference display distinct target selection dynamics. J. Neurosci. *33*, 9520–9529.

Lennert, T., Cipriani, R., Jolicoeur, P., Cheyne, D., and Martinez-Trujillo, J.C. (2011). Attentional modulation of neuromagnetic evoked responses in early human visual cortex and parietal lobe following a rank-order rule. J. Neurosci. *31*, 17622–17636.

Mante, V., Sussillo, D., Shenoy, K.V., and Newsome, W.T. (2013). Context-dependent computation by recurrent dynamics in prefrontal cortex. Nature *503*, 78–84.

Marois, R., and Ivanoff, J. (2005). Capacity limits of information processing in the brain. Trends Cogn. Sci. *9*, 296–305.

Miller, E.K., and Cohen, J.D. (2001). An integrative theory of prefrontal cortex function. Annu. Rev. Neurosci. *24*, 167–202.

Mitchell, J.F., Sundberg, K.A., and Reynolds, J.H. (2007). Differential attention-dependent response modulation across cell classes in macaque visual area V4. Neuron *55*, 131–141.

Mitchell, J.F., Sundberg, K.A., and Reynolds, J.H. (2009). Spatial attention decorrelates intrinsic activity fluctuations in macaque area V4. Neuron *63*, 879–888.

Monosov, I.E., and Thompson, K.G. (2009). Frontal eye field activity enhances object identification during covert visual search. J. Neurophysiol. *102*, 3656–3672.

Moore, T., and Armstrong, K.M. (2003). Selective gating of visual signals by microstimulation of frontal cortex. Nature *421*, 370–373.

Moore, T., and Fallah, M. (2004). Microstimulation of the frontal eye field and its effects on covert spatial attention. J. Neurophysiol. *91*, 152–162.

Moore, T., Armstrong, K.M., and Fallah, M. (2003). Visuomotor origins of covert spatial attention. Neuron *40*, 671–683.

Moran, J., and Desimone, R. (1985). Selective attention gates visual processing in the extrastriate cortex. Science *229*, 782–784.

Moreno-Bote, R., Beck, J., Kanitscheider, I., Pitkow, X., Latham, P., and Pouget, A. (2014). Information-limiting correlations. Nat. Neurosci. *17*, 1410–1417.

Müller, J.R., Philiastides, M.G., and Newsome, W.T. (2005). Microstimulation of the superior colliculus focuses attention without moving the eyes. Proc. Natl. Acad. Sci. USA *102*, 524–529.

Musallam, S., Corneil, B.D., Greger, B., Scherberger, H., and Andersen, R.A. (2004). Cognitive control signals for neural prosthetics. Science *305*, 258–262.

Newsome, W.T., Britten, K.H., and Movshon, J.A. (1989). Neuronal correlates of a perceptual decision. Nature *341*, 52–54.

Niebergall, R., Khayat, P.S., Treue, S., and Martinez-Trujillo, J.C. (2011). Multifocal attention filters targets from distracters within and beyond primate MT neurons' receptive field boundaries. Neuron *72*, 1067–1079.

Nienborg, H., and Cumming, B. (2010). Correlations between the activity of sensory neurons and behavior: how much do they tell us about a neuron's causality? Curr. Opin. Neurobiol. *20*, 376–381.

Nienborg, H., Cohen, M.R., and Cumming, B.G. (2012). Decision-related activity in sensory neurons: correlations among neurons and with behavior. Annu. Rev. Neurosci. *35*, 463–483.

Niven, J.E., and Laughlin, S.B. (2008). Energy limitation as a selective pressure on the evolution of sensory systems. J. Exp. Biol. *211*, 1792–1804.

Noudoost, B., and Moore, T. (2011). Control of visual cortical signals by prefrontal dopamine. Nature *474*, 372–375.

Noudoost, B., Chang, M.H., Steinmetz, N.A., and Moore, T. (2010). Top-down control of visual attention. Curr. Opin. Neurobiol. *20*, 183–190.

Opris, I., Hampson, R.E., Gerhardt, G.A., Berger, T.W., and Deadwyler, S.A. (2012). Columnar processing in primate pFC: evidence for executive control microcircuits. J. Cogn. Neurosci. *24*, 2334–2347.

Petersen, S.E., and Posner, M.I. (2012). The attention system of the human brain: 20 years after. Annu. Rev. Neurosci. *35*, 73–89.

Petrides, M. (2005). Lateral prefrontal cortex: architectonic and functional organization. Philos. Trans. R. Soc. Lond. B Biol. Sci. *360*, 781–795.

Posner, M.I. (1980). Orienting of attention. Q. J. Exp. Psychol. *32*, 3–25.

Posner, M.I., Cohen, Y., and Rafal, R.D. (1982). Neural systems control of spatial orienting. Philos. Trans. R. Soc. Lond. B Biol. Sci. *298*, 187–198.

Pouget, P., Stepniewska, I., Crowder, E.A., Leslie, M.W., Emeric, E.E., Nelson, M.J., and Schall, J.D. (2009). Visual and motor connectivity and the distribution of calcium-binding proteins in macaque frontal eye field: implications for saccade target selection. Front. Neuroanat. *3*, 2.

Rainer, G., Asaad, W.F., and Miller, E.K. (1998). Selective representation of relevant information by neurons in the primate prefrontal cortex. Nature *393*, 577–579.

Rigotti, M., Barak, O., Warden, M.R., Wang, X.-J., Daw, N.D., Miller, E.K., and Fusi, S. (2013). The importance of mixed selectivity in complex cognitive tasks. Nature *497*, 585–590.

Rizzolatti, G., Riggio, L., Dascola, I., and Umiltá, C. (1987). Reorienting attention across the horizontal and vertical meridians: evidence in favor of a premotor theory of attention. Neuropsychologia *25* (1A), 31–40.

Rochel, O., and Cohen, N. (2007). Real time computation: zooming in on population codes. Biosystems *87*, 260–266.

Sanger, T.D. (2003). Neural population codes. Curr. Opin. Neurobiol. *13*, 238–249.

Schafer, R.J., and Moore, T. (2011). Selective attention from voluntary control of neurons in prefrontal cortex. Science *332*, 1568–1571.

Shadlen, M.N., and Newsome, W.T. (1994). Noise, neural codes and cortical organization. Curr. Opin. Neurobiol. *4*, 569–579.

Shadlen, M.N., and Newsome, W.T. (1998). The variable discharge of cortical neurons: implications for connectivity, computation, and information coding. J. Neurosci. *18*, 3870–3896.

Shadlen, M.N., Britten, K.H., Newsome, W.T., and Movshon, J.A. (1996). A computational analysis of the relationship between neuronal and behavioral responses to visual motion. J. Neurosci. *16*, 1486–1510.

Squire, R.F., Noudoost, B., Schafer, R.J., and Moore, T. (2013). Prefrontal contributions to visual selective attention. Annu. Rev. Neurosci. *36*, 451–466.

Stokes, M.G., Kusunoki, M., Sigala, N., Nili, H., Gaffan, D., and Duncan, J. (2013). Dynamic coding for cognitive control in prefrontal cortex. Neuron *78*, 364–375.

Suzuki, M., and Gottlieb, J. (2013). Distinct neural mechanisms of distractor suppression in the frontal and parietal lobe. Nat. Neurosci. *16*, 98–104.

Takeda, K., and Funahashi, S. (2002). Prefrontal task-related activity representing visual cue location or saccade direction in spatial working memory tasks. J. Neurophysiol. *87*, 567–588.

Thompson, K.G., and Bichot, N.P. (2005). A visual salience map in the primate frontal eye field. Prog. Brain Res. *147*, 251–262.

Thompson, K.G., Bichot, N.P., and Sato, T.R. (2005a). Frontal eye field activity before visual search errors reveals the integration of bottom-up and top-down salience. J. Neurophysiol. *93*, 337–351.

Thompson, K.G., Biscoe, K.L., and Sato, T.R. (2005b). Neuronal basis of covert spatial attention in the frontal eye field. J. Neurosci. *25*, 9479–9487.

Tolhurst, D.J., Movshon, J.A., and Dean, A.F. (1983). The statistical reliability of signals in single neurons in cat and monkey visual cortex. Vision Res. *23*, 775–785.

Tomko, G.J., and Crapper, D.R. (1974). Neuronal variability: non-stationary responses to identical visual stimuli. Brain Res. *79*, 405–418.

Treue, S., and Martínez Trujillo, J.C. (1999). Feature-based attention influences motion processing gain in macaque visual cortex. Nature *399*, 575–579.

Wardak, C., Ibos, G., Duhamel, J.-R., and Olivier, E. (2006). Contribution of the monkey frontal eye field to covert visual attention. J. Neurosci. *26*, 4228–4235.

Womelsdorf, T., Fries, P., Mitra, P.P., and Desimone, R. (2006). Gamma-band synchronization in visual cortex predicts speed of change detection. Nature *439*, 733–736.